

Angular dependence of the critical currents in Mo₇₇Ge₂₃/Ge multilayers

S. de Brion, W. R. White, A. Kapitulnik, and M. R. Beasley
Edward L. Ginzton Laboratory, Stanford University, Stanford, California 94305

(Received 4 January 1994)

We examine the critical current densities of superconducting/insulating Mo₇₇Ge₂₃/Ge multilayers in magnetic fields applied at arbitrary angles with respect to the superconducting layers. In these measurements, we demonstrate the existence of a threshold field, below which the critical current is governed only by the perpendicular component of the applied field. Also, we observe that there exists a critical angle that divides two different regimes of vortex pinning. Finally, we relate these results to existing theories of vortices in layered superconductors.

INTRODUCTION

Since the discovery of the high-temperature superconductors, there has been renewed interest in layered superconductors, especially their vortex state properties. In this paper, we present a study of the angular dependence of the critical currents J_c in superconducting/insulating (S/I) amorphous Mo₇₇Ge₂₃/Ge multilayers in an applied magnetic field. These multilayers are an effective model system to study vortices in layered superconductors, since the coupling strength between the superconducting planes can be varied easily by simply changing the Ge thickness. Our samples range from barely coupled quasi-two-dimensional superconductors to highly coupled, slightly anisotropic bulk superconductors.

From our study, we find two characteristic features of the angular dependence of J_c in such layered systems. First, there exists a threshold field below which the critical current is governed only by the perpendicular component of the magnetic field. Second, there also exists a critical angle that delimits two different regimes in the vortex pinning. We will discuss these results within the framework of existing theories of vortices in layered structures.

EXPERIMENTS

Thin-film multilayers of amorphous Mo₇₇Ge₂₃/Ge were deposited by multitarget magnetron sputtering on amorphous Si₃N₄/Si substrates.¹ The thickness d_s of the superconducting Mo₇₇Ge₂₃ layers was maintained constant and equal to 60 Å. The insulating Ge thickness d_i was varied from 125 Å down to 15 Å. The multilayers contained a total of ten superconducting layers. From previous work, we know that these multilayers have a well-defined layered structure with a sharp S/I interface.² The critical temperature, for all the samples, was 5.4 K.

The bulk properties of amorphous superconducting Mo₇₇Ge₂₃ are well known. Its penetration depth is 7700 Å at 0 K and its coherence length 55 Å. Due to the amorphous nature of the superconductor, pinning is moderate, with $J_c \approx 10^4$ A/cm² at low temperatures and

high fields.

The multilayers were patterned by reactive ion etching into structures of length 2.54 mm and width 20 μm suitable for four-point electrical measurement. The critical current was measured using a dc voltage criterion of 5 μV. The corresponding current density was calculated using the total Mo₇₇Ge₂₃ thickness only, since amorphous Ge is not conducting. A magnetic field was applied perpendicular to the current, and the angle φ it made with the layers ($\varphi=0$ being parallel) was varied from -90° to $+90^\circ$. The magnitude of the field ranged from 40 Oe up to 6 kOe. By comparison, the lower and upper critical fields H_{c1} and H_{c2} for bulk Mo₇₇Ge₂₃ are 15 Oe and 35 kOe, respectively, at 4.2 K. All the measurements presented have been made at 4.2 K unless otherwise specified. A summary of the material parameters of the samples is given in Table I. The mass ratio M/m for sample *MG35/10b* was determined from conductivity measurements: The fluctuation conductivity was fit to the Lawrence-Doniach model, from which we extracted the anisotropy ratio. For the other samples, M/m was obtained by extrapolation from the *MG35/10b* value using the difference in insulator thicknesses and the measured Josephson coupling length of 8 Å in amorphous Ge. The perpendicular coherence length ξ_\perp was then deduced from the mass ratio, assuming that the parallel coherence length is the same as that of bulk Mo₇₇Ge₂₃: 55 Å at zero temperature and 117 Å at 4.2 K [using a temperature dependence $(1-T/T_c)^{-1/2}$]. From these estimates, we can infer the degree of coupling in each sample. These are compared in the bottom row of the table.

We have also evaluated the London penetration depth for currents flowing within the film plane using the bulk value $\lambda_0=7700$ Å at 0 K and its evaluation at 4.2 K using a $(1-T/T_c)^{-1/2}$ temperature dependence. Since λ_0 is larger than the sample thickness d_t , the actual penetration depth is the so-called perpendicular penetration depth: $\lambda_\perp=\lambda_0^2/d_t$. Due to the layered structure, an additional correction is introduced to account for the electrons being distributed in the whole sample volume.³ We then obtain $\lambda_\perp=(\lambda_0^2/d_t)\sqrt{(d_s+d_i)/d_s}$. The other parameters given in Table I will be discussed later.

TABLE I. Summary of the material parameters of the samples.

Sample	MG125/10b	MG35/10	MG25/10b	MG15/10
d_i	125 Å	35 Å	25 Å	15 Å
d_s	60 Å	60 Å	60 Å	60 Å
d_t	1850 Å	950 Å	850 Å	750 Å
M/m	∞	16	5	1.5
ξ_1 (at 4.2 K)		28 Å	52 Å	96 Å
λ_1 (at 4.2 K)	68.8 μm	96.0 μm	102.0 μm	108.0 μm
$H_{c\parallel}$ (at 4.2 K)		1.2 kG	2.8 kG	3.6 kG
H_{Th} (at 4.2 K)		~ 0.8 G	~ 2 kG	~ 3 kG
φ_0 0 K		60°	57°	
4.2 K		40°	36°	
φ_x		14°	24°	
	decoupled layers	Josephson coupled layers $\xi_1 < d_i$	Josephson coupled layers $d_i < \xi_1$ $< d_i + d_s$	Anisotropic G-L superconductor or $\xi_1 > d_i + d_s$

RESULTS

The critical currents observed for the four different samples are presented in Figs. 1–4. The critical current density J_c is plotted as a function of the perpendicular component of the applied field, $H_{\text{perp}} = H_a \sin\varphi$. For most cases, the data were taken by varying φ at fixed H_a . By contrast, the curves labeled $J(H_{a\perp})$ show J_c as a func-

tion of the magnitude of H_a when H_a was applied only perpendicular to the multilayers, i.e., for $\varphi = \pi/2$. In going from Fig. 1 to Fig. 4, one sees how J_c changes as a function of H_{perp} as the insulating thickness is decreased, and correspondingly, the coupling increased.

In Fig. 1 the data for the largest insulating thickness ($d_i = 125$ Å) are plotted. The inset shows the angular dependence of J_c at different fields, from 55 Oe to 5 kOe.

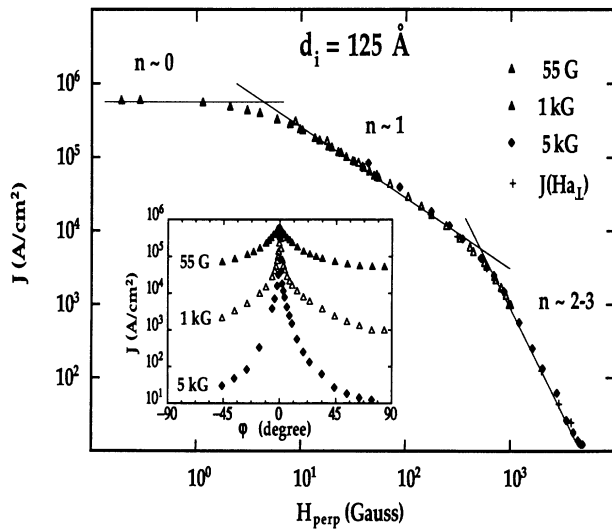


FIG. 1. Critical current density J_c as a function of the perpendicular component H_{perp} of the applied magnetic field for sample MG125/10b. Inset: J_c as a function of the angle φ between the applied field and the sample layers.

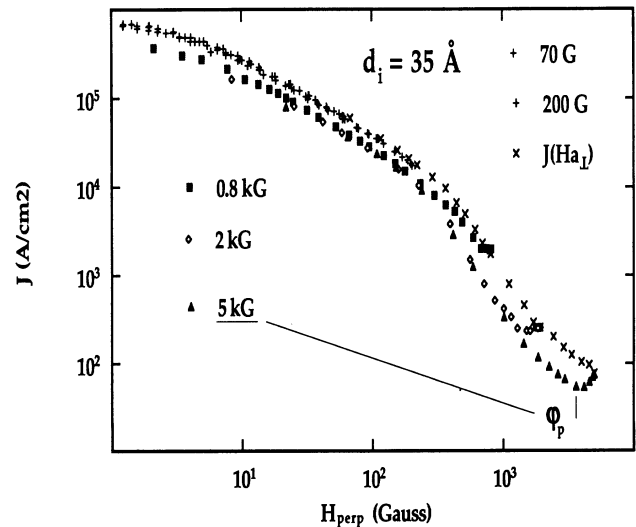


FIG. 2. Critical current density J_c as a function of the perpendicular component H_{perp} of the applied magnetic field for sample MG35/10.

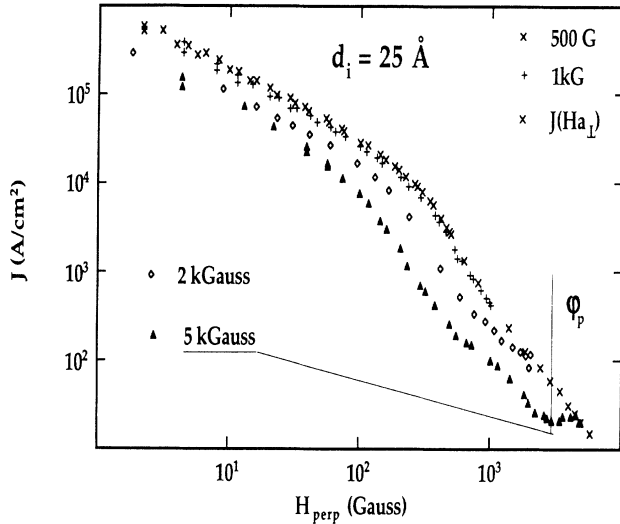


FIG. 3. Critical current density J_c as a function of the perpendicular component H_{perp} of the applied magnetic field for sample $MG25/10b$.

There is a sharp increase in J_c when the magnetic field approaches the parallel direction. The plot of J_c versus H_{perp} is more revealing: When plotted this way, all the curves collapse onto a single universal curve, showing that J_c depends only on H_{perp} . This is expected for superconducting layers with no Josephson coupling, i.e., $M/m = \infty$. In this case, the parallel component of the magnetic field is unscreened and 2D pancake vortices³⁻⁷ form in each superconducting layer. Only the relatively weak magnetic interaction remains and tends to align the pancake vortices along the perpendicular direction. Moreover, $J(H_{a\perp})$ and $J_c(H_{\text{perp}})$ are identical, as they should be.

Such complete universal behavior is no longer observed

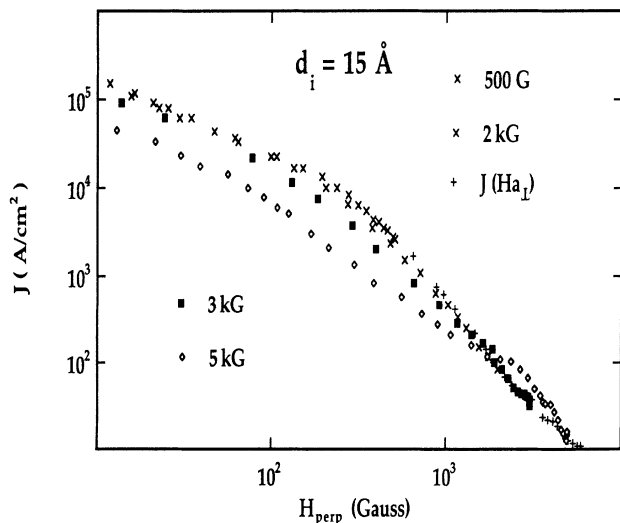


FIG. 4. Critical current density J_c as a function of the perpendicular component H_{perp} of the applied magnetic field for sample $MG15/10$.

in the other samples where the Ge thickness is reduced to 35, 25, and 15 Å. In these samples, universal behavior is observed only at low fields, and in this regime $J_c(H_{\text{perp}}) = J(H_{a\perp})$. For example, in Fig. 2 the data for $H_a = 70$ and 200 Oe fall on a universal curve, whereas the data for $H_a \geq 0.8$ kOe are displaced to lower values of J_c at a given H_{perp} . A similar trend is seen in Figs. 3 and 4. In all cases, the displaced curves bend over and join the $J(H_{a\perp})$ curve at $H_{\text{perp}} = H_a$, i.e., when $\varphi = \pi/2$, as they should. The threshold fields H_{Th} above which the data begin to deviate from universal behavior given by $J(H_{a\perp})$, are listed in the table. As can be seen, H_{Th} depends on d_i , increasing as d_i decreases and the interlayer coupling increases. We return to the interpretation of H_{Th} below.

Looking at the field dependence of $J(H_{a\perp})$, a common trend for all the samples is observed. The magnitude of $J(H_{a\perp})$ differs slightly from one sample to the other (it is the biggest for $MG35/10$ and the smallest for $MG15/10$) reflecting possibly small differences in the pinning in the individual layers or some intrinsic dependence on anisotropy. In any event, the field dependence is the same. Three regimes can be distinguished which may be approximately characterized by $J_c \propto H^{-n}$ in each, but corresponding to different values of n . Referring for example to Fig. 1, at the highest fields, $n \approx 2-3$, crossing over to $n \approx 1$ as the field decreases. The crossover field $H \approx 300$ Oe corresponds to a vortex lattice parameter $a_0 \approx (\Phi_0/B)^{1/2}$ of the order of 2500 Å. The third regime where $n \approx 0$ arises at the lowest fields, $H < 2$ Oe.

The existence of a regime in which J_c is proportional to H^{-1} raises the question whether or not this is an artifact of the measurement: At low fields, the constant voltage criterion used to determine J_c might be too big, causing the sample to be biased in the flux-flow regime, in which case changes in the flux-flow resistivity $R_{\text{ff}} \propto H$ might cause perceived changes in J_c . We have eliminated this possibility by measuring the flux-flow resistivity at higher fields and extrapolating back to these small fields. The corresponding current necessary to produce a voltage of 5 μV is negligible compared to the measured critical current. Therefore the crossover observed at $H \approx 300$ Oe reflects a change in pinning.

From single-film measurements,⁸ we know that at high fields above 1 kG, the pinning of vortices is collective and that the two-dimensional theory of collective pinning proposed by Larkin and Ovchinnikov⁹ should apply, at least qualitatively. However, as H_a is reduced, we expect the vortices increasingly to become pinned individually. The crossover should occur when $R_c \approx a_0$. We can roughly estimate the corresponding magnetic field: From Ref. 9 we get $R_c \approx (a_0 c_{66} / B J_c)^{1/2}$ where c_{66} is the vortex lattice shear modulus. Using the evaluation of c_{66} similar to the one performed in Ref. 8 for a single film and taking the observed high-field dependence of J_c in $MG125/10b$, we obtain a crossover field of the order of 300 Oe. This is consistent with the observed field at which n changes from 2-3 to 1. On the other hand, $n = 1$ corresponds to a field-dependent pinning force for individual vortices, the origin of which are not obvious.

The crossover to the third regime as the field is further

decreased can be understood unambiguously and does not reflect a change in pinning. It is a consequence of the self-field of the applied current. The high current passing through the sample (several mA) produces its own magnetic field that can dominate the total field. This self-field at the edge of the film is given by $B_s \approx (\mu_0 I / 2\pi w) \ln(2w/d_t)$, where I is the applied current, d_t the sample thickness, and w its width. For our samples, at the highest critical current, $I \approx 2$ mA, this gives $H_s \approx 2$ Oe, which is what is observed experimentally. The observed critical current remains constant for $H_a < 2$ Oe. The dependence of B_s on I and w was also checked on a wider sample. The crossover to single pinning of vortices should occur at lower fields. Indeed $a_0 \approx \lambda$ corresponds to a field of 0.5 Oe for sample *MG125/10b*, for instance.

Due to this self-field effect and the fact that demagnetization effects are important in our geometry, we would not expect to observe the lock-in of vortices^{5,10} in these films as $\varphi \rightarrow 0$, even if the anisotropy were high enough in principle.

Let us consider now the field dependence of J_c for the coupled samples when $H_a > H_{Th}$. For *MG35/10*, starting from the perpendicular direction (large H_{perp}), J_c initially remains constant or even decreases as H_{perp} decreases, corresponding to H_a deviating from the perpendicular direction. J_c then once again scales as H_{perp} , but its value is displaced from $J(H_{a1})$, as we have already noted.

When the insulating thickness is decreased to 25 Å (sample *MG25/10b*, Fig. 3), we still observe a constant J_c starting from the perpendicular direction; but, at large deviations, scaling with H_{perp} is no longer observed. For *MG15/10* where $d_i = 15$ Å, the angular dependence is much more complicated, and it is clear that H_{perp} is no longer a sufficient variable to characterize the data.

To gain some insight into the nature of this minimum in $J_c(H_{perp})$, we have determined from the data the actual angle φ_p at which the minimum arises for any given H_a (see for example Fig. 2). It is plotted in Fig. 5 as a function of the applied magnetic field for the sample

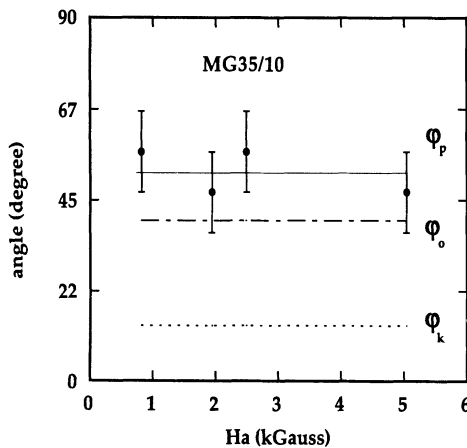


FIG. 5. φ_p as a function of the applied magnetic field for sample *MG35/10*. Also plotted are the calculated values of φ_0 and φ_k .

MG35/10. We see that φ_p has a constant value $\varphi_p \approx 48^\circ$ independent of H_a . This constant value is, however, temperature dependent. It increases when the temperature is lowered: at 1.5 K, $\varphi_p \approx 70^\circ$. The same kind of behavior is observed in sample *MG25/10b* in which the insulating thickness is reduced to 25 Å (see Fig. 3). However when the insulating thickness is further decreased to 15 Å (sample *MG15/10*), $J_c(H_{perp})$ does not exhibit a minimum and φ_p is no longer defined.

From the above considerations, we see that these experiments lead to two important generalizations. First, there exists a threshold field below which J_c depends only on H_{perp} . This is a common characteristic of all the coupled samples. Second, there exists a field independent angle φ_p at which $J_c(H_{perp})$ is minimized. As we now show, these results can be correlated with specific aspects of structures in layered superconductors.

INTERPRETATION

When the superconducting layers of a multilayer are sufficiently well coupled, the superconducting coherence length in the perpendicular direction exceeds the periodicity of the multilayer. Then the superconductor can be treated as a whole and described within the frame work of the Ginzburg-Landau theory, introducing a mass tensor to account for the anisotropy.¹¹ Sample *MG15/10* falls into this category.

In the other limit where the superconducting layers are widely separated, the superconducting order parameter is confined to the superconducting layers. *Pancake* vortices form^{4,6} in these layers. The magnetic interaction from one plane to the other tends to align these two-dimensional (2D) vortices according to the perpendicular component of the applied field, but no currents flow from layer to layer. Hence, the parallel component remains unscreened. Sample *MG125/10b* is in this limit. The critical current density depends on H_{perp} only. Bismuth based high-temperature superconductors are probably also in this category, because the same kind of behavior for $J_c(H_{perp})$ is indeed observed.^{6,12,13}

Between these two limits, for small but non-negligible Josephson coupling, a discrete layered approach is more appropriate: the Lawrence-Doniach model¹⁴ should then be used to describe the system. The phase difference of the superconducting order parameter between layers varies on the Josephson length scale $r_j = d\sqrt{M/m}$, where d is the periodicity of the layered structure. For example, $r_j = 380$ Å in *MG35/10* and 190 Å in *MG25/10b*. When the applied field is tilted, different kinds of vortices may occur depending on the angle between the magnetic field and the layers.^{3,5} Three different regimes occur which are governed by the distance $1 = d \cdot \text{tg}(\pi/2 - \varphi)$ separating two coupled *pancake* vortices on adjacent layers.

For very slight tilts, $1 < \xi_{||}$ and the 3D London theory applies. For larger tilts, $\xi_{||} < 1 < r_j$, and the 3D London theory is valid only at distances greater than 1; the domain between $\xi_{||}$ and 1 is referred to as the 2D core. Finally, when $1 > r_j$, a Josephson string forms connecting the 2D cores: The vortices have a staircase-shaped struc-

ture and are called *kinked* vortices.

There are two characteristic angles separating these three regimes: φ_0 , given by $\text{tg}(\pi/2 - \varphi_0) = \xi_{\parallel}/d$, and φ_k , given by $\text{tg}(\pi/2 - \varphi_k) = r_j/d = \sqrt{M/m}$. In each of these regimes, the structure of the vortices is sufficiently different that different regimes of behavior are to be expected. In particular, for the line energy of a single vortex, deviations from the London model become more significant for $\varphi < \varphi_0$.⁵

These two new angles, φ_0 and φ_k , are compared with our empirically determined φ_p in Fig. 5. It is clear that the minimum in $J_c(H_{\text{perp}})$ is associated with φ_0 . This means that there is a change in pinning when the 2D vortex cores from adjacent layers are separated by more than a coherence length.

We now turn to one possible explicit interpretation of the minimum observed in J_c vs H_{perp} . It is known that edge pinning occurs in our samples.⁸ It is intuitively obvious that edge pinning will depend on the angle of the field with respect to the superconducting layers.

Edge pinning can be understood using the concept of image vortices. 3D-like Abrikosov vortices encounter the Bean-Livingston surface barrier¹⁵ that prevents them from entering the sample when the applied magnetic field is smaller than $H_s \approx H_c$. But in our layered films, disklike vortices may enter the sample at much lower fields. Mints and Shapiro¹⁶ have calculated the energy of a vortex disk as a function of the distance the disk penetrates into the sample. Above a certain applied field $H_1 \approx H_{c1}$ ($H_{c1\perp}$ for our sample configuration), the free energy has a maximum beyond which it decreases to become negative with a minimum at a distance x_m from the surface. The authors suggest that disklike vortices enter the sample by thermal activation and reside randomly in the vicinity of a plane defined by $x = x_m$ from the edge. A process of this general sort may occur in our samples where H_1 probably does not exceed a few tenths of Oersted. Taking for example sample *MG35/10* at 1 kG, we obtain a barrier energy on the order of 1 K, which, at 4.2 K, can be overcome by thermal agitation. We also calculate $x_m \approx 100 \mu\text{m}$. This is larger than the sample width, demonstrating the need for a more complete theory. Clearly both surfaces would have to be considered to obtain a more reasonable result for our case. The omitted Josephson coupling effect should also be included.

Additional insight into edge barriers as the possible origin of the minimum in J_c can be obtained as follows. Consider a vortex aligned along the applied field formed from a line of coupled 2D pancake vortices. Each pancake vortex feels an edge barrier. For H_a perpendicular to the film, the vortex is parallel to the edge and each pancake vortex feels an identical edge barrier, i.e., a kind of surface or coupled edge barrier. For H_a tipped at an angle, some vortices penetrate the edge of the film and enter the bulk of the film. These vortices still feel an edge barrier, but it is greatly reduced in strength because only those pancake vortices near the point of penetration are near enough to the edge to feel a strong edge barrier. Thus there is some critical angle beyond which the edge barrier loses effectiveness.

In the less coupled sample, with $d_i = 35 \text{ \AA}$, at angles

smaller than φ_p , the critical current starts to scale with the perpendicular component of the magnetic field. This is in agreement with the existence of *kinked* vortices: The Josephson vortices are strongly pinned in the insulating layers and all the dissipation arises from the *pancake* vortices moving within the superconducting layers. In our experimental configuration, the force acting on the Josephson vortices (i.e., the strings) is directed perpendicular to the layers, whereas for the 2D vortices it remains in the superconducting planes.

When the Ge thickness is decreased to 25 \AA , sample *MG25/10b*, edge pinning is probably still present when the magnetic field is applied perpendicular to the layers. It becomes less efficient when the field is tilted and disappears at φ_0 in the same way as in *MG35/10*. However the scaling with the perpendicular component of the field at lower angles does not occur in *MG25/10b*. We note here that the insulating thickness is smaller than the perpendicular coherence length, which means that the Josephson vortex is not confined to the insulator layer. It is no longer completely locked in the insulator. Its movement may cause some additional field-dependent dissipation.

For the sample *MG15/10* (Fig. 4), it is obvious that the perpendicular component of the magnetic field is no longer a good parameter. This sample can be considered as an anisotropic Ginzburg-Landau superconductor: No pancake vortices nor kinked vortices are likely to form.

Let us return now to the threshold field H_{Th} below which J_c remains equal to J_{perp} . The physical origin of this field can be understood if we recall that our films are thin compared to the superconducting penetration depth so that the lower critical field for the parallel direction $H_{c1\parallel}$ is enhanced due to finite film thickness effects. The calculation of $H_{c1\parallel}$ for a thin film includes an infinite row of image vortices on each side of the film.¹⁷ For our coupled multilayer samples, we must take into account the anisotropy so that

$$H_{c1\parallel} = \frac{2\Phi_0}{\pi\mu_0} \frac{1}{\sqrt{M/m}} \frac{1}{d_i} \ln \left(\frac{d_i}{\xi_{\perp}} \right),$$

where Φ_0 is the flux quantum, M/m is the mass ratio, d_i the total thickness of the film, and ξ_{\perp} the perpendicular coherence length. ξ_{\perp} must be replaced by the insulating thickness d_i if the latter is smaller.

The calculated values for $H_{c1\parallel}$ are given in Table I. The plot of H_{Th} versus $H_{c1\parallel}(d)$ in Fig. 6 gives clear evidence that H_{Th} and $H_{c1\parallel}$ are related. A fit of the data leads to $H_{\text{Th}} \approx 0.75H_{c1\parallel}$. The reduction of H_{Th} below $H_{c1\parallel}$ is likely due in this picture to the angular dependence of H_{c1} .

We can then interpret the results for the coupled samples as follows: When the magnetic field has a magnitude smaller than $H_{c1}(\varphi)$, the parallel component of the magnetic field cannot enter the sample; the vortex structure is hence determined by the perpendicular component of the field only, so that $J_c(H, \varphi)$ depends on H_{perp} and is the same as $J_c(H, \varphi=0)$.

A related question arises in the presence of such a high critical field $H_{c1\parallel}$: Does this critical field also prevent the

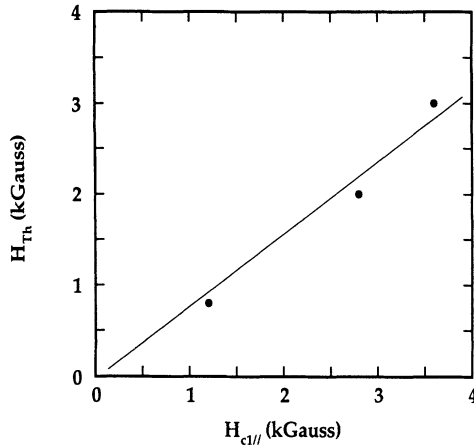


FIG. 6. Threshold field H_{Th} as a function of the calculated lower critical field $H_{c1//}$ for samples *MG35/10*, *MG25/10b*, and *MG15/10*.

“parallel” parts of the kinked vortices from forming until the parallel component of the applied field has reached $H_{c1//}$? For two independent vortex lattices, one given by the parallel component of the applied field, the other one by its perpendicular component, such a behavior could occur. In our films, however, this is not the case. None of our measurements of J_c plotted as a function of the parallel component of the applied field $H_a \sin\phi$ show a change of behavior when $H_a \sin\phi \approx H_{c1//}$. Thus, in our samples, the vortices do not form independent parallel and perpendicular lattices. Indeed, Bulaevskii, Ledvij, and Kogan⁵ predict that such combined vortices should occur only when $\lambda < r_j$, which is not the case for all of our samples.

CONCLUSION

We have measured $\text{Mo}_{77}\text{Ge}_{23}/\text{Ge}$ multilayers with different Ge thicknesses. For widely separated superconducting layers, the critical current depends only on the perpendicular component of the magnetic field. This can be explained by neglecting the Josephson coupling between the layers: *pancake* vortices form according to the perpendicular component of the field, while the parallel one remains unscreened.

For smaller insulating thicknesses ($d_i \leq 35 \text{ \AA}$), Josephson coupling is important. There exists a threshold field H_{Th} below which only the perpendicular component of the applied magnetic field enters the sample. This threshold field, H_{Th} , is related to the small sample thickness and to anisotropy. We have established a correlation between this threshold critical field and $H_{c1//}$.

We have also established the existence of a field-independent critical angle ϕ_p at which $J_c(H_{\text{perp}})$ is minimum and changes its behavior as a function of angle. It appears correlated with ϕ_0 , the angle at which 2D vortices from different layers are separated by one coherence length. ϕ_p disappears when the insulating Ge thickness of the sample has been reduced to 15 \AA . Our results are consistent with expectations based on the existence of edge pinning.

ACKNOWLEDGMENTS

This work was supported by the Joint Services Electronics Program, the Air Force Office of Scientific Research, and benefited from the facilities of the NSF-MRL supported Center for Materials Science.

- ¹J. M. Graybeal, Ph.D. thesis, Stanford University, 1985 (unpublished).
- ²V. Matijasevic and M. R. Beasley, *Phys. Rev. B* **35**, 3175 (1987).
- ³D. Feinberg, *Physica C* **194**, 126 (1992).
- ⁴J. Clem, *Phys. Rev. B* **43**, 7873 (1991).
- ⁵L. N. Bulaevskii, M. Ledvij, and V. G. Kogan, *Phys. Rev. B* **46**, 366 (1992).
- ⁶P. H. Kes, J. Aarts, V. M. Vinokur, and C. J. van der Beek, *Phys. Rev. Lett.* **64**, 1063 (1990).
- ⁷M. Tachiki and S. Takahashi, *Solid State Commun.* **72**, 1083 (1989).
- ⁸W. R. White, A. Kapitulnik, and M. R. Beasley, *Phys. Rev. Lett.* **70**, 670 (1993).
- ⁹A. I. Larkin and Yu. N. Ovchinnikov, *J. Low Temp. Phys.* **34**,

409 (1979).

- ¹⁰D. Feinberg and C. Villard, *Phys. Rev. Lett.* **65**, 919 (1990).
- ¹¹V. L. Ginzburg, *Zh. Eksp. Teor. Fiz.* **23**, 236 (1952).
- ¹²H. Raffy, S. Labdi, O. Laborde, and P. Monceau, *Phys. Rev. Lett.* **66**, 2515 (1991).
- ¹³P. Schmitt, P. Kummeth, L. Schultz, and G. Saemann-Ischenko, *Phys. Rev. Lett.* **67**, 267 (1991).
- ¹⁴W. E. Laurence and S. Doniach, in *Proceedings of the Twelfth International Conference on Low Temperature Physics*, edited by E. Kanda (Academic Press of Japan, Kyoto, 1971), p. 361.
- ¹⁵C. P. Bean and D. J. Livingstone, *Phys. Rev. Lett.* **12**, 14 (1964).
- ¹⁶R. G. Mints and I. B. Shapiro (unpublished).
- ¹⁷T. P. Orlando and K. A. Delin, *Foundation of Applied Superconductivity* (Addison-Wesley, Reading, MA, 1991).